

# Design and Analysis of Asymmetric Rotor Pole Type Bearingless Switched Reluctance Motor

Zhenyao Xu, *Member, CES and IEEE*, Qingguo Yu, *Member, CES*,  
and Fengge Zhang, *Member, CES and IEEE*

**Abstract**—Bearingless switched reluctance motor (BSRM) not only combines the merits of bearingless motor (BM) and switched reluctance motor (SRM), but also decreases the vibration and acoustic noise of SRM, so it could be a strong candidate for high-speed driving fields. Under the circumstances, a 12/14 BSRM with hybrid stator pole has been proposed due to its high output torque density and excellent decoupling characteristics between torque and suspension force. However, this motor has torque dead-zone, which leads to problems of self-start at some rotor positions and large torque ripple during normal operation. To solve the existing problems in the 12/14 type, an asymmetric rotor pole type BSRM is proposed. The structure and design process of the proposed motor is presented in detail. The characteristics of the proposed motor is analyzed and compared with that of the 12/14 type. Furthermore, prototype of the proposed structure is designed, manufactured and experimented. Finally, simulation and test results are illustrated and analyzed to prove the validity of the proposed structure.

**Index Terms**—Asymmetric rotor pole, bearingless switched reluctance motor, self-start, torque ripple reduction.

## I. INTRODUCTION

HIGH-SPEED switched reluctance motor (SRM) has a broad application prospect in high-speed drive equipment fields due to its simple structure and flexible control. Although the existing high-speed SRM could solve the problems of mechanical bearing, such as wear and heating, by magnetic bearing technology, the magnetic bearing only plays the role of suspension and support in the motor and does not produce any torque, and its existence increases the axial length of the motor, resulting in the decrease in critical speed of the rotor.

Bearingless switched reluctance motor (BSRM) combines technologies of bearingless motor (BM) and SRM, so it not only inherits merits of BM and SRM, but also effectively

decreases the vibration and acoustic noise of SRM. Hence, BSRM is a strong candidate for high-speed drive field [1].

At present, the traditional BSRM structures are mainly researched, including 12/8 double winding type [2]-[4], 12/8 single winding type [5]-[8], and 8/6 single winding type [9]. Although the rotor of these structures could be controlled stably at center position regardless of the rotor stationary or rotating, they have serious coupling problems between torque and suspension force control, it not only affects the torque and suspension force control performance of the motor, but also greatly increases the motor control difficulty.

For reducing coupling degree between the torque and suspension force control of traditional BSRMs, many BSRMs with improvement structures are proposed.

In terms of rotor structure improvement of BSRMs, scholars proposed hybrid rotor type [10] and wide rotor pole type [11]-[12] BSRMs. Compared with traditional BSRMs, hybrid rotor type and wide rotor type BSRMs can improve the suspension force performance of the motor to a certain extent, but they still have coupling problems between torque and suspension force control.

In terms of stator structure improvement of BSRM, scholars proposed 12/8 sharing suspension windings type BSRMs [13]-[14]. Although the BSRMs with sharing suspension windings basically realize the natural decoupling of torque and suspension force control, their structures are complex and the radial suspension force still has a great coupling between the x- and y-directions in the motors. In the meantime, scholars also proposed 8/10, 12/14 and 12/12 hybrid stator pole type BSRMs [15]-[17]. These three motor structures realize the natural decoupling of torque and suspension force control, and the suspension forces in the x- and y-directions are also basically decoupled. However, these three motors have torque dead-zone in some rotor positions, in which the motor could not self-start, and the torque ripple in these motors is slightly larger when the motor is in normal operation.

In this paper, an asymmetric rotor type BSRM is proposed to settle the problems of self-start and large torque ripple in the 12/14 BSRM with hybrid stator pole. Firstly, structure and design process of the proposed motor is introduced. Then, the characteristics of the proposed motor are obtained by finite element method (FEM) and compared to that of 12/14 hybrid rotor type. Finally, prototype of the proposed motor is designed and manufactured, and the simulation and test results are illustrated and analyzed to prove the validity of the proposed structure.

Manuscript received January 31, 2022; revised February 10, 2022. accepted February 17, 2021. date of publication March 25, 2022; date of current version March 18, 2022.

This work was supported by National Natural Science Foundation of China under Grant 52077141 and 51920105011, Young and Middle-Aged Scientific and Technological Innovation Talent Program of Shenyang City of Liaoning Province of China under Grant RC200427.

(Corresponding Author: Zhenyao Xu)

Z. Xu is with Shenyang University of Technology, Shenyang, 110870, China (e-mail: zhenyao87@163.com).

Q. Yu is with Shenyang University of Technology, Shenyang, 110870, China (e-mail: 1424048123@qq.com).

F. Zhang is with Shenyang University of Technology, Shenyang, 110870, China (e-mail: zhangfg@stu.edu.cn).

Digital Object Identifier 10.30941/CESTEMS.2022.00002

## II. STRUCTURE OF ASYMMETRIC ROTOR POLE TYPE BSRM

### A. Conventional 12/14 BSRM

Fig. 1 gives the structure of conventional 12/14 BSRM. It consists of stator, rotor, shaft, torque windings and suspension windings. The stator adopts hybrid stator pole structure, including torque and suspension pole. The torque pole, the narrower stator pole, is designed for generating torque. The suspension pole, the wider stator pole, is designed for generating suspension force. The torque and suspension windings are wound on the torque and suspension poles, respectively. The torque windings, which are wound on torque poles  $P_{A1}$ ,  $P_{A2}$ ,  $P_{A3}$  and  $P_{A4}$ , respectively, are connected in series to form phase A, and the torque windings, which are wound on torque poles  $P_{B1}$ ,  $P_{B2}$ ,  $P_{B3}$  and  $P_{B4}$ , respectively, are connected in series to form phase B. The suspension windings, which are wound on suspension poles  $P_{xp}$ ,  $P_{yp}$ ,  $P_{xn}$  and  $P_{yn}$ , become one phase, respectively. The rotor employs a salient pole structure, and its 14 poles are evenly distributed on the circumference of the rotor. Inside the rotor is the shaft.

Fig. 2 shows torque profiles of conventional 12/14 BSRM. In the figure, the position of zero rotor angle is defined at the alignment position of phase B winding axis and rotor tooth axis. When the rotor is parked near the rotor position of 0, 13 or 26 degrees, the torque of the motor is close to zero, which is called torque dead-zones. If the rotor is parked within these regions, the motor could not be able to complete self-start. In addition,

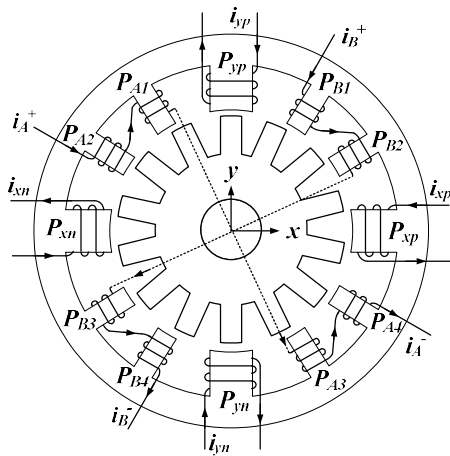


Fig. 1. Structure of conventional 12/14 BSRM.

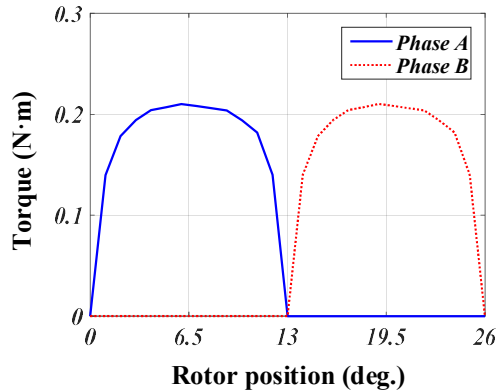


Fig. 2. Torque profiles of conventional 12/14 BSRM.

when the motor is running normally, the motor will have a large torque ripple due to the exceptionally small output torque near the rotor position of 0, 13 or 26 degrees, and the torque ripple cannot be decreased no matter what control strategy is employed.

### B. Asymmetric Rotor Pole Type BSRM

In order to solve the problems of self-start and large torque ripple of conventional 12/14 BSRM, the torque equation of SRM is analyzed. Generally, the output torque  $T$  of an SRM could be calculated by the phase inductance  $L$ , phase current  $i$  and rotor position  $\theta$  as,

$$T = \frac{1}{2} i^2 \frac{dL}{d\theta} \quad (1)$$

in which,  $L$  could be expressed as,

$$L = \frac{\mu_0 \mu_r N^2 A}{g} = \frac{\mu_0 \mu_r N^2 L_{stk} R}{g} (\theta_o + K_{fr}) \quad (2)$$

in which,  $\mu_0$  is vacuum permeability,  $\mu_r$  is relative permeability,  $N$  is number of windings turns,  $L_{stk}$  is stack length of the core,  $R$  is rotor radius,  $g$  is air gap length,  $\theta_o$  is overlap angle,  $K_{fr}$  is leakage inductance constant. It can be seen from (2) that the phase inductance  $L$  could be affected by many parameters.

The conventional 12/14 BSRM is a two-phase motor, with a stepping angle of 12.85 degrees or half the rotor pole pitch. Therefore, to eliminate the torque dead-zone of the motor, improving the starting torque and decreasing torque ripple of the motor, the positive torque period produced by each phase of the conventional 12/14 BSRM has to be wider than 12.85 degree. In other words, the change rate of inductance of torque windings of the conventional 12/14 BSRM has to be wider than 12.85 degree. According to (2), the phase inductance  $L$  of the motor winding is inversely proportional to the air gap length  $g$ . If the air gap length of the conventional 12/14 BSRM could be changed with rotor position, it is very possible to generate a positive torque with the period wider than 12.85 degree, thereby eliminating the torque dead-zone. Builds upon this idea, an asymmetric rotor pole type BSRM is proposed in Fig. 3. The only difference between the conventional 12/14 BSRM and proposed structure is that the rotor pole surface of the proposed motor has a structure similar to a step.

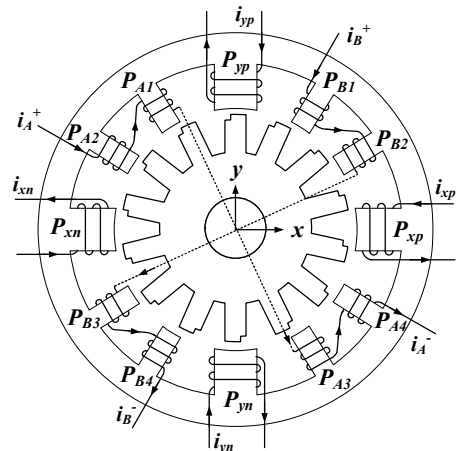


Fig. 3. Structure of asymmetric rotor pole type BSRM.

### III. DESIGN OF ASYMMETRIC ROTOR POLE TYPE BSRM

To verify the effectiveness of the proposed structure, this paper designs the proposed motor based on the structure of conventional 12/14 BSRM. During the design process, most parameters of the conventional 12/14 BSRM are retained, and only the shapes of torque and rotor poles are redesigned.

#### A. Selection of Pole Arc

The proposed motor is a double salient pole motor, so the selection of the torque and rotor pole arc is very important, which directly affects the performance of the motor. In order for the proposed motor to be self-start at any rotor position, it is required that the motor could generate electromagnetic torque at any rotor position. That is, the inductance curves of adjacent phases of the motor must have some overlap in ascending period, as shown in Fig. 4. However, it should be noted that increasing the self-starting capacity of the motor may have a certain impact on the output torque of the motor, so a compromise between starting and average torque of the motor should be considered carefully during the design of the proposed motor.

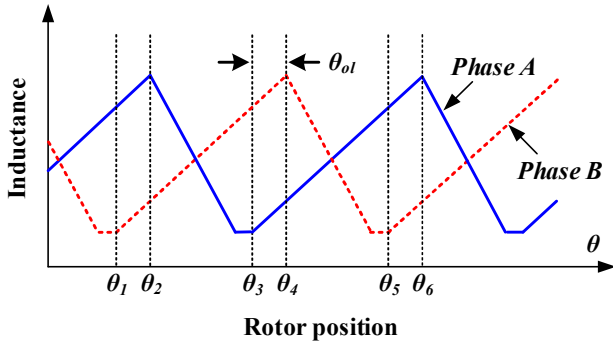


Fig. 4. Diagram of inductance overlap angle.

Fig. 5 shows the main parameters in asymmetric rotor pole type BSRM.  $\beta_{st}$  is pole arc of torque pole,  $\beta_{sf}$  is pole arc of suspension pole,  $\beta_r$  is pole arc of the asymmetric rotor pole,  $\beta_{rs}$  is step angle of the asymmetric rotor pole, and  $h_{rs}$  is step height of the asymmetric rotor pole. To settle the self-starting problem and decrease the torque ripple in conventional 12/14 BSRM, at the same time keeping the average torque production capacity not much decreased compared with that of conventional 12/14 BSRM, the pole arcs of torque and rotor poles of the proposed motor should meet the following requirements:

$$\beta_r > \frac{360^\circ}{qN_r} = \frac{360^\circ}{2 \times 14} \approx 12.85^\circ \quad (3)$$

$$\beta_{st} + \beta_r \leq \frac{360^\circ}{N_r} = \frac{360^\circ}{14} \approx 25.7^\circ \quad (4)$$

$$\beta_{st} < \beta_r \quad (5)$$

in which,  $N_r$  is number of rotor poles,  $q$  is number of phases of motor. According to (3), (4) and (5), the available value range of  $\beta_{st}$  and  $\beta_r$  could be determined as red shadow area in Fig. 6.

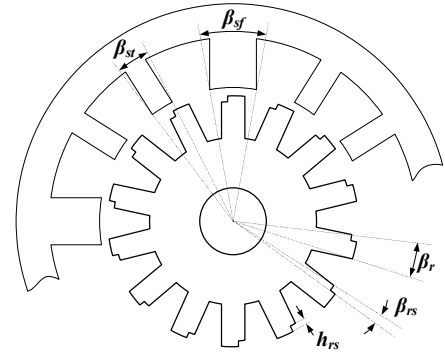


Fig. 5. Parameters in asymmetric rotor pole type BSRM.

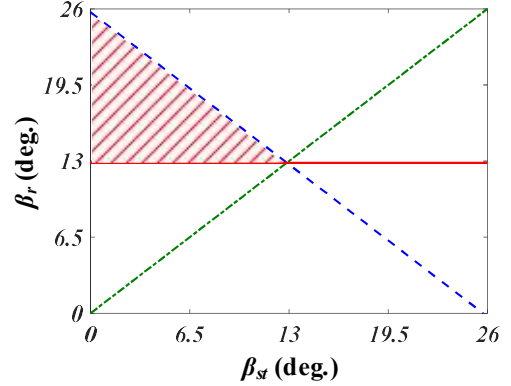


Fig. 6. Available value range for  $\beta_{st}$  and  $\beta_r$ .

The torque and suspension force are particularly important for BSRM, and their performance is directly related to the success or failure of BSRM design. Therefore, in the design of the proposed BSRM, it is necessary to consider not only the self-starting capacity and torque ripple of the motor, but also the output torque and suspension force performance of the motor.

According to Fig. 6, several feasible combinations of  $\beta_{st}$  and  $\beta_r$  are selected, and FEM is used to simulate the motor structure of each combination. During the simulation, the magnetomotive force (MMF) is kept the same for each combination of  $\beta_{st}$  and  $\beta_r$ . At the same time, to ensure the correctness and fairness of simulation results, the maximum magnetic flux density of the motor should be kept below 1.8T, which is close to the properties of the actual core material. If it is found that the maximum magnetic flux density of a certain combination of  $\beta_{st}$  and  $\beta_r$  exceeds 1.8T, the combination of  $\beta_{st}$  and  $\beta_r$  will be eliminated immediately.

TABLE I and II give the average torque and suspension force of the motor under the feasible combination of  $\beta_{st}$  and  $\beta_r$ . As can be seen from TABLE I, when  $\beta_r$  is fixed, the average torque of the motor decreases significantly with the decrease of  $\beta_{st}$ . When  $\beta_{st}$  is constant, the change of the average torque of the motor is not obvious with  $\beta_r$  increasing. From TABLE II it can be seen that when  $\beta_r$  is fixed, the average suspension force of the motor does not change significantly with  $\beta_{st}$  decreasing, vice versa. Therefore, consider self-start, output torque and suspension capacity of the motor, three groups of combinations of  $\beta_{st}$  and  $\beta_r$ ,  $12^\circ/13.5^\circ$ ,  $11^\circ/14^\circ$  and  $10^\circ/14.5^\circ$  respectively, are selected as the initial values of the next motor design.

TABLE I

AVERAGE TORQUE OF THE MOTOR WITH VARIOUS POLE ARC COMBINATION OF TORQUE AND ROTOR POLES (N·M)

$\beta_{st}$	$\beta_r$		
	13.5°	14°	14.5°
12°	0.170	—	—
11°	0.167	0.163	—
10°	0.159	0.159	0.152
9°	0.150	0.149	0.145

TABLE II

AVERAGE SUSPENSION FORCE OF THE MOTOR WITH VARIOUS POLE ARC COMBINATION OF TORQUE AND ROTOR POLES (N)

$\beta_{st}$	$\beta_r$		
	13.5°	14°	14.5°
12°	53.475	—	—
11°	52.840	54.525	—
10°	52.167	53.810	55.521
9°	51.449	53.067	54.743

### B. Selection of Step Angle

Step angle and height are important parameters of asymmetric rotor pole structure. Changing their size could change the inductance characteristics of torque windings of the proposed motor, and thus indirectly change the torque and suspension force of the motor.

On the basis of the selection of combination of  $\beta_{st}$  and  $\beta_r$  in previous section, with the step height fixed at 0.2mm, the available step angle for each selected combination of  $\beta_{st}$  and  $\beta_r$  are evaluated as shown in Figs. 7 to 9. In the figures,  $T_{max}$  is maximum torque,  $T_{av}$  is average torque,  $T_{st}$  is starting torque,  $T_{min}$  is minimum torque,  $T_{ripple}$  is torque ripple.

Fig. 7 shows that, compared with other combinations of  $\beta_{st}$ ,  $\beta_r$  and  $\beta_{rs}$ , the combination of  $\beta_{st}=12^\circ$ ,  $\beta_r=13.5^\circ$  and  $\beta_{rs}=1.5^\circ$  could produce the maximum starting torque and average torque, and the torque ripple is the smallest. It can be seen from Fig. 8 that the starting and average torque produced by the combination of  $\beta_{st}=11^\circ$ ,  $\beta_r=14^\circ$  and  $\beta_{rs}=3^\circ$  are not the maximum values, but its starting and average torque values are close to the maximum values, and this combination has the smallest torque ripple, so this combination is considered as the optimal combination in Fig. 8. Similarly, it could be concluded from Fig. 9 that the combination of  $\beta_{st}=10^\circ$ ,  $\beta_r=14.5^\circ$  and  $\beta_{rs}=4.5^\circ$  is the optimal combination.

In order to select the optimal combination of  $\beta_{st}$ ,  $\beta_r$  and  $\beta_{rs}$ , this paper compares  $T_{st}$ ,  $T_{max}$ ,  $T_{min}$ ,  $T_{av}$  and  $T_{ripple}$  of the three optimal combinations obtained from Figs. 7 to 9, as shown in Fig. 10. The comparison results show that the combination of  $\beta_{st}=11^\circ$ ,  $\beta_r=14^\circ$  and  $\beta_{rs}=3^\circ$  is the best combination of the three combinations, because this combination has lower torque ripple, higher starting and average torque.

### C. Selection of Step Height

Fig. 11 shows the torque characteristics of the motor at different step heights. It can be seen from the figure that when the step height is 0.2mm, the motor has the largest average torque, the smallest torque ripple and the second largest starting torque. Therefore, step height 0.2mm is the best option for the proposed structure.

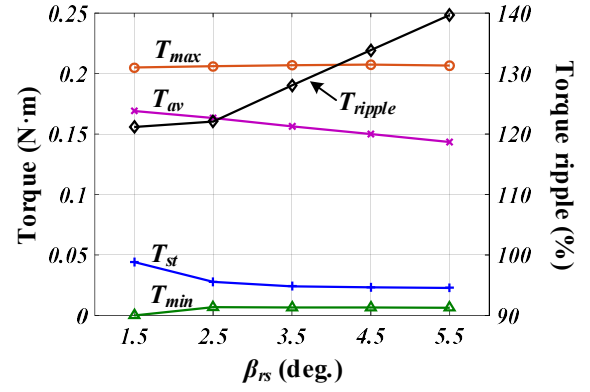
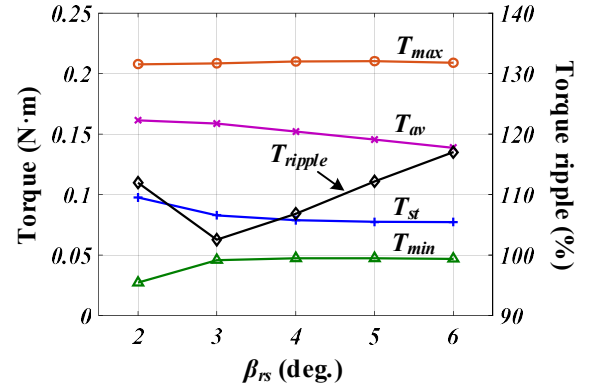
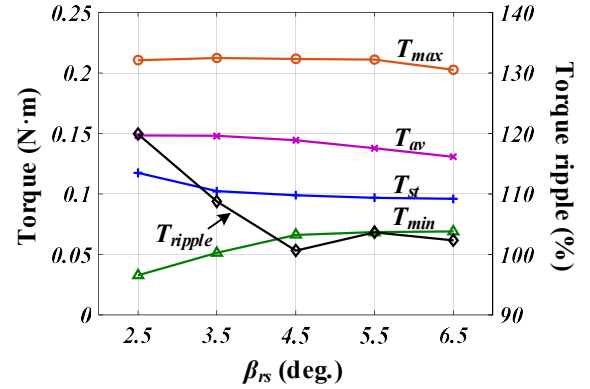
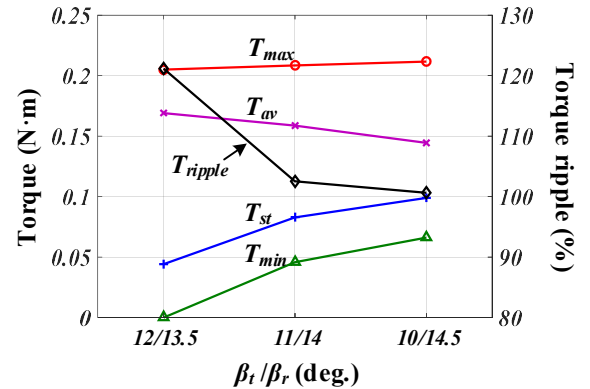
Fig. 7. Torque characteristics with various step angle ( $\beta_{st}=12^\circ$ ,  $\beta_r=13.5^\circ$ ).Fig. 8. Torque characteristics with various step angle ( $\beta_{st}=11^\circ$ ,  $\beta_r=14^\circ$ ).Fig. 9. Torque characteristics with various step angle ( $\beta_{st}=10^\circ$ ,  $\beta_r=14.5^\circ$ ).

Fig. 10. Torque characteristics comparison with various torque and rotor pole arc.

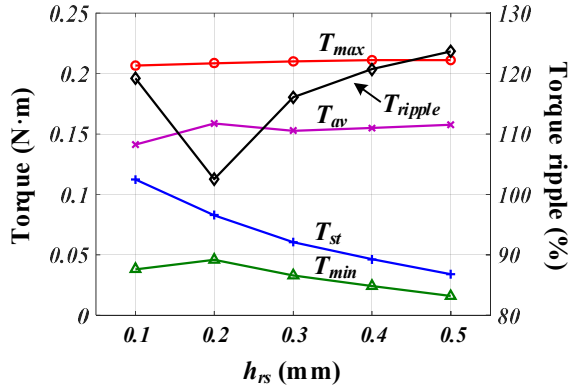


Fig. 11. Torque characteristics with variant step height.

#### D. Parameters of Proposed BSRM

According to the aforementioned analysis and discussion, the parameters of the proposed motor are designed as shown in TABLE III.

TABLE III  
PARAMETERS OF CONVENTIONAL AND PROPOSED BSRMS

Parameters	Conventional	Proposed
Stator outer diameter (mm)	112	112
Stator yoke thickness (mm)	7.7	7.7
Stator inner diameter (mm)	60.2	60.2
Air gap (mm)	0.3	0.3
Rotor yoke thickness (mm)	9.7	9.7
Shaft diameter (mm)	18	18
Stack length (mm)	40	40
Suspension pole arc (deg.)	25.7	25.7
Torque pole arc (deg.)	12.85	11
Rotor pole arc (deg.)	12.85	14
Step angle (deg.)	—	3
Step height (mm)	—	0.2
Torque winding turns per pole	80	80
Suspension winding turns per pole	100	100

### IV. CHARACTERISTICS ANALYSIS OF ASYMMETRIC ROTOR POLE TYPE BSRM

To prove the validity of the proposed structure, FEM is used to obtain the inductance, torque and suspension force characteristics of conventional and proposed BSRMs.

#### A. Inductance Characteristics

Fig. 12 shows the inductance characteristics of torque windings in conventional and proposed BSRMs. Compared with conventional BSRM, the inductance in the proposed BSRM is smaller, while its ascending period is wider, this is caused by asymmetric rotor pole structure, in which there is a step at the beginning of the rotor pole. Furthermore, the wider inductance ascending period in the proposed BSRM is good for settling the problems of self-start and large torque ripple in conventional BSRM.

Fig. 13 shows the inductance characteristics of suspension windings in conventional and proposed BSRMs. It could be found that the inductance in the two BSRMs changes slightly with respect to rotor position. This mainly owes to the hybrid stator pole structure of the two BSRMs, in which the overlap area of the suspension and rotor pole is always the same

regardless of rotor position. Moreover, the inductance in the proposed BSRM is slightly smaller than that of conventional BSRM, which is caused by the step at the beginning of the asymmetric rotor poles.

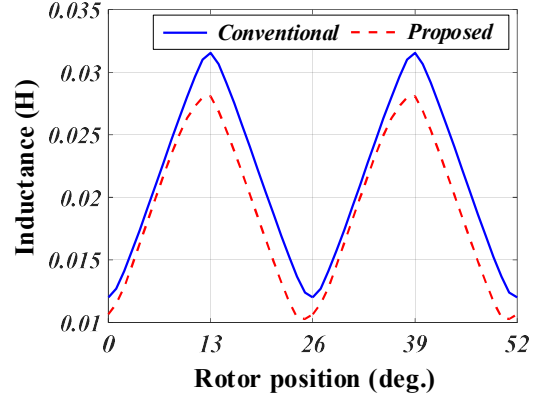


Fig. 12. Inductance characteristics of torque windings.

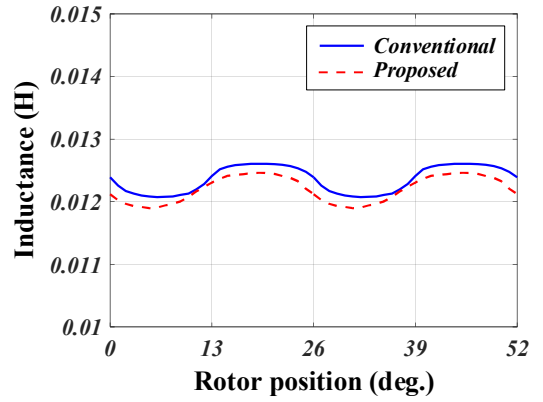


Fig. 13. Inductance characteristics of suspension windings.

#### B. Torque Characteristics

Fig. 14 shows the torque characteristics between conventional and proposed BSRMs. Figs. 15 to 17 show the average torque, starting torque and torque ripple in conventional and proposed BSRMs, respectively. Compared to conventional type, the proposed structure could eliminate the torque dead zone and produce positive torque at any rotor position. Furthermore, although the average torque of the proposed structure is slightly lower than that of conventional 12/14 BSRM, the proposed structure increases starting torque and decreases torque ripple, which meets the goal of proposed motor, proving the effectiveness of the proposed motor.

#### C. Suspension Force Characteristics

Fig. 18 shows suspension force characteristics of conventional and proposed BSRMs. Windings on the suspension pole  $P_{yp}$  of the two BSRMs are excited, respectively. As the current is constant, the suspension force in the two BSRMs has excellent linearity with rotor position, which is beneficial to suspension control of the rotor. However, the average suspension force produced by the proposed motor is slightly decreased compared to that of conventional one as shown in Fig. 19, because of the asymmetric rotor poles.



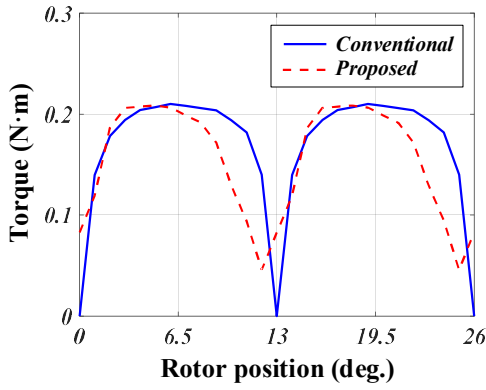


Fig. 14. Torque characteristics of conventional and proposed BSRMs.

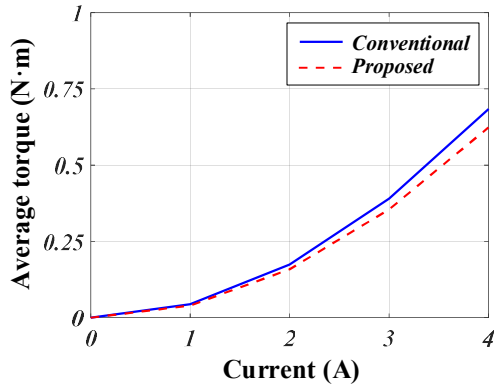


Fig. 15. Average torque in conventional and proposed BSRMs.

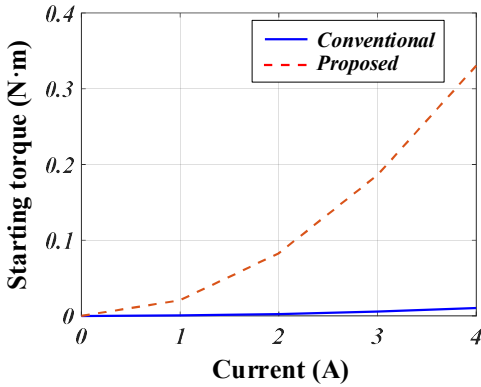


Fig. 16. Starting torque in conventional and proposed BSRMs.

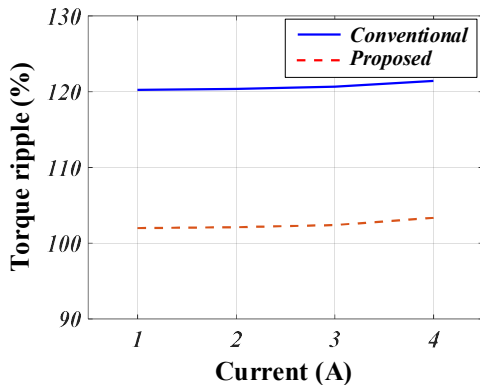


Fig. 17. Torque ripple in conventional and proposed BSRMs.

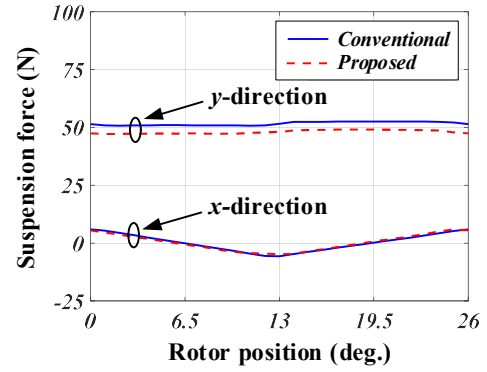


Fig. 18. Suspension force characteristics of conventional and proposed BSRMs.

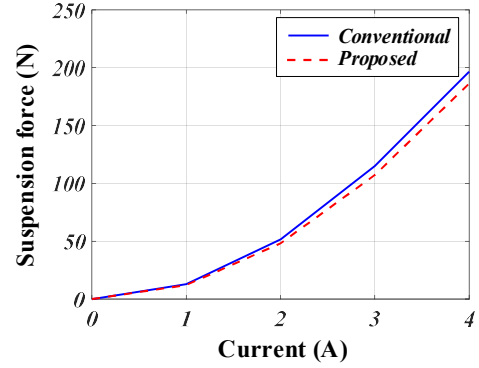


Fig. 19. Average suspension force in conventional and proposed BSRMs.

#### D. Decoupling Characteristics

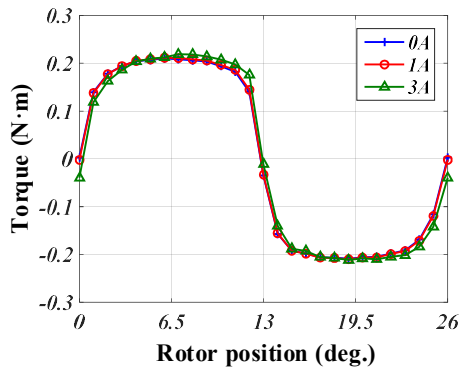
Fig. 20 shows torque profiles of conventional and proposed BSRMs with fixed torque winding current ( $i_A=2A$ ) and various suspension winding currents. It can be found that the effect of the suspension winding currents on torque is very small in the two types, which could be ignored if compared with the torque produced by the torque winding current.

Fig. 21 shows suspension force profiles of conventional and proposed BSRMs with fixed suspension winding current ( $i_{yp}=2A$ ) and various torque winding currents. The effect of torque winding currents on the suspension force is also very small in the two types, it could be ignored if compared with the suspension force produced by the suspension winding current.

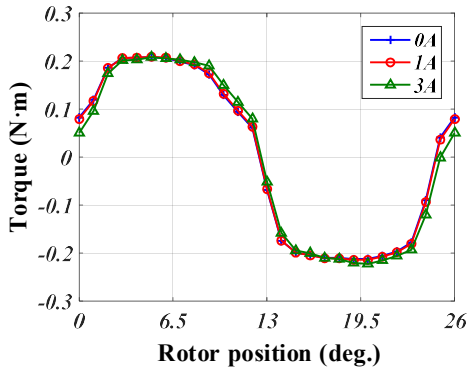
On the basis of the above-mentioned analysis, it concludes that the proposed BSRM not only inherits the excellent characteristics of conventional 12/14 BSRM, namely the natural decoupling between torque and suspension force control, but also solves the problems of self-start and large torque ripple in conventional 12/14 BSRM, which proves the effectiveness of the proposed structure.

## V. EXPERIMENTAL RESULTS

A prototype of the proposed BSRM is designed and manufactured as shown in Fig. 22. The experimental results of the proposed BSRM with suspension force control at 1000rpm is shown in Fig. 23. Without suspension force control, the rotor rotates eccentrically. With suspension force control, the rotor could be pulled back center position rapidly and stable operation in center position, which proves the validity of the proposed BSRM.

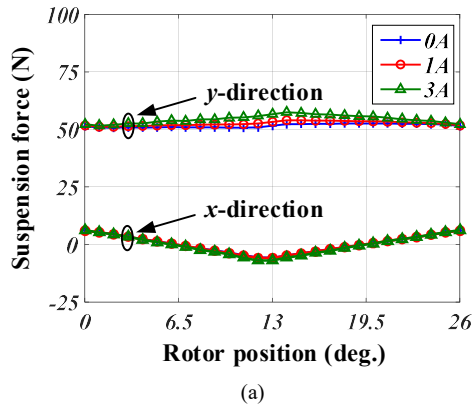


(a)

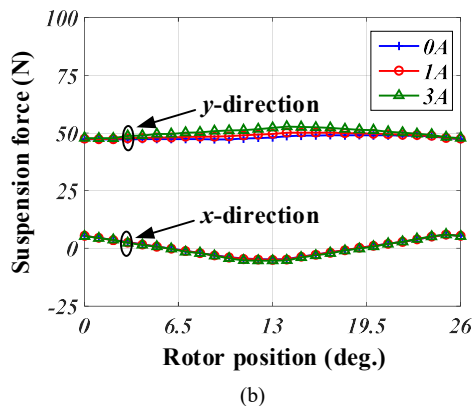


(b)

Fig. 20. Torque profiles of the two BSRMs with fixed torque winding current ( $i_t=2A$ ) and various suspension winding currents. (a) Conventional. (b) Proposed.



(a)



(b)

Fig. 21. Suspension force profiles of the two BSRMs with fixed suspension winding current ( $i_{sp}=2A$ ) and various torque winding currents. (a) Conventional. (b) Proposed.

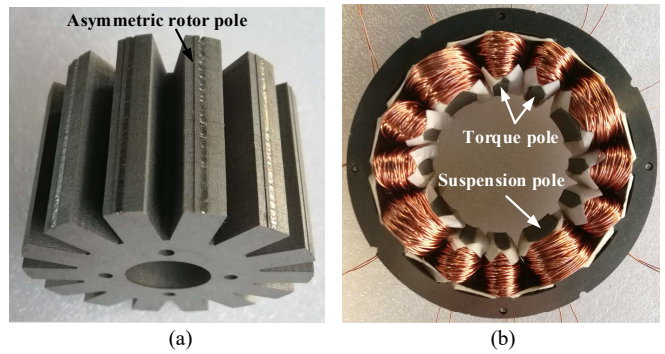
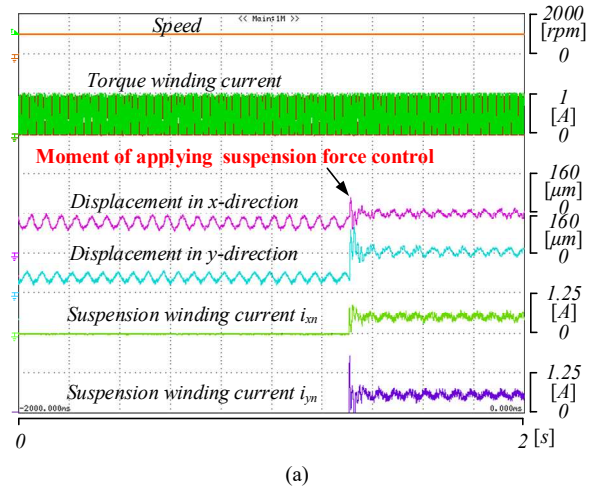
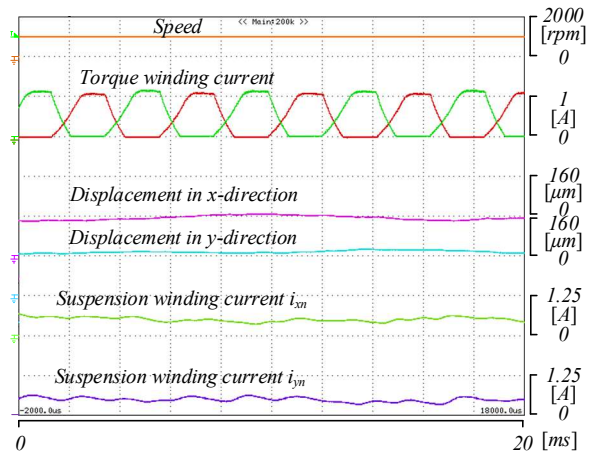


Fig. 22. Prototype of proposed BSRM. (a) Rotor. (b) Stator.



(a)



(b)

Fig. 23. Experimental results of the proposed BSRM with rotor rotating at 1000rpm. (a) Suddenly apply suspension force control. (b) Enlarge view of stable suspension force control.

## VI. CONCLUSIONS

In this paper, an asymmetric rotor pole type BSRM is proposed to settle the problems of self-starting and large torque ripple in the conventional 12/14 BSRM. To prove the effectiveness and feasibility, the proposed motor is designed, manufactured and tested. The characteristics of conventional 12/14 and proposed BSRMs are analyzed and compared. The comparison results show that the starting and minimum torque of the proposed motor could exceed 80mN·m and 45mN·m, respectively, and they are about 0mN·m in conventional 12/14

BSRM. The torque ripple of the proposed motor is approximately 20% lower than that of conventional 12/14 BSRM. The decoupling characteristics are almost same as that of conventional 12/14 BSRM. Therefore, the proposed motor not only inherits the excellent decoupling characteristics of conventional 12/14 BSRM, but also settles the self-starting problems and decreases torque ripple of conventional 12/14 BSRM.

#### REFERENCES

- [1] S. Ayari, M. besbes, M. Lecrivain, and M. Gabsi, "Effectes of the air gap eccentricity on the SRM Vibrations," in *Proc. Int. Conf. Electr. Mach. and Drives*, 1999, pp.138-140.
- [2] M. Takemoto, H. Suzuki, A. Chiba, et al., "Improved analysis of a bearingless switched reluctance motor," *IEEE Trans. Ind. Application*, vol. 37, no. 1, pp. 26-34, Feb. 2001.
- [3] X. Cao, Z. Deng, G. Yang, et al., "Independent control of average torque and radial force in bearingless switched-reluctance motors with hybrid excitations," *IEEE Transactions on Power Electronics*, vol. 24, no. 5, pp. 1376-1385, 2009.
- [4] M. Takemoto, A. Chiba, H. Suzuki, et al., "Radial force and torque of a bearingless switched reluctance motor operating in a region of magnetic saturation," *IEEE Trans. Ind. Application*, vol. 40, no. 1, pp. 103-112, 2004.
- [5] F. C. Lin, S. M. Yang, "Self-bearing control of a switched reluctance motor using sinusoidal currents," *IEEE Trans. Power Electron.*, vol. 22, no. 6, pp. 2518-2526, 2007.
- [6] X. Cao, H. Yang, L. Zhang and Z. Deng, "Compensation strategy of levitation forces for single-winding bearingless switched reluctance motor with one winding total short circuited," *IEEE Transactions on Industrial Electronics*, vol. 63, no. 9, pp. 5534-5546, Sept. 2016.
- [7] X. Cao, J. Zhou, C. Liu, et al., "Advanced control method for a single-winding bearingless switched reluctance motor to reduce torque ripple and radial displacement," *IEEE Transactions on Energy Conversion*, vol. 32, no. 4, pp. 1533-1543, 2017.
- [8] Z. Hao, Q. Yu, X. Cao, X. Deng and X. Shen, "An improved direct torque control for a single-winding bearingless switched reluctance motor," *IEEE Transactions on Energy Conversion*, vol. 35, no. 3, pp. 1381-1393, Sept. 2020.
- [9] L. Chen, W. Hofman, "Speed regulation technique of one bearingless 8/6 switched reluctance motor with simpler single winding structure," *IEEE Transactions on Industrial Electronics*, vol. 59, no. 6, pp. 2592-2600, June 2012.
- [10] C. R. Morrison, M. W. Siebert and E. J. Ho, "Electromagnetic forces in a hybrid magnetic-bearing switched-reluctance motor," *IEEE Trans. on Magnetics*, vol.44, no.12, December 2008.
- [11] Y. Yang, F. Liu, C. Liu, "A new bearingless switched reluctance motor with wide rotor pole arc," in *Proceedings of 9th Conference on Industrial Electronics and Applications (ICIEA 2014)*, 2014, pp. 374-378.
- [12] J. Zhou, Z. Deng, X. Cao, et al., "Decoupling mechanism of torque and levitation-force control for 12/4 dual-winding bearingless switched reluctance motor," in *Proceedings of 19th International Conference on Electrical Machines and Systems (ICEMS 2016)*, 2016, pp. 1-6.
- [13] Y. Yang, Z. Liu, Z. Deng, "Performance analysis of a new type bearingless switched reluctance motor," *Small and Special Electrical Machines*, vol. 42, no. 11, pp. 14-17, 2014.
- [14] X. Wang, R. Cui, Y. Hao, Y. Liu and P. Zhao, "Radial force model of a bearingless switched reluctance motor with sharing suspension windings considering magnetic saturation," *Electric Machines and Control*, vol. 25, no. 6, pp. 46-53, June 2021.
- [15] D. H. Lee and J. W. Ahn, "Design and analysis of hybrid stator bearingless SRM," *Journal of Electrical Engineering & Technology*, vol. 6, no. 1, pp. 94-103, 2011.
- [16] Z. Xu, D. H. Lee, J. W. Ahn, "Comparative analysis of bearingless switched reluctance motors with decoupled suspending force control," *IEEE Transactions on Industry Applications*, vol. 51, no. 1, pp. 733-743, 2015.
- [17] H. Wang, J. Liu, J. Bao, et al, "A novel bearingless switched reluctance

motor with biased permanent magnet," *IEEE Transactions on Industrial Electronics*, vol. 61, no. 12, pp. 6947-6955, 2014.



**Zhenyao Xu** (M'14) was born in Liaoning, China, in 1987. He received the B.S. and M.S. degrees in electrical engineering from Shenyang University of Technology, Shenyang, China, in 2009 and 2012, respectively, and the M.S. and Ph.D degrees in mechatronics engineering from Kyungsoong University, Busan, South Korea, in 2012 and 2016, respectively.

He worked in mechatronics engineering as an Assistant Professor in 2016 with Kyungsoong University. From 2017 to 2018, he was an Assistant Professor with the State Key Laboratory of Robotics, Shenyang Institute of Automation, the Chinese Academy of Sciences. Since 2018, he has been with School of Electrical Engineering, Shenyang University of Technology, Shenyang, China, as an Associate Professor. His research interests include electrical machines and their control systems.



**Qingguo Yu** was born in Liaoning, China, in 1997. He received the B.S. degree in electrical engineering from Dalian Jiaotong University in 2019. He is currently pursuing the M.S. degree in electrical engineering from Shenyang University of Technology since 2019.

His research interests include electric motors and their control systems.



**Fengge Zhang** (M'17) received the B.S., M.S., and Ph.D. degrees in electrical engineering from Shenyang University of Technology, Shenyang, China, in 1984, 1990, and 2000, respectively.

He worked in School of Electrical Engineering, Shenyang University of Technology since 1984. From 2001 to 2002, he has been with Esslingen University of Applied Sciences, Esslingen, Germany, as a Visiting Scholar. His research interests include motor design and control, and wind power generation system.